

Contribution from the Department of Chemistry, North Carolina State University, Raleigh, North Carolina 27650,
Department of Chemistry, The University of North Carolina at Charlotte, Charlotte, North Carolina 28223,
and Naval Research Laboratory, Washington, D.C. 20375

Redox and Spectral Properties of Nickel(II) Macrocycles Containing Dianionic, Tetraazaannulene Ligands

CYNTHIA L. BAILEY,[†] ROBERT D. BEREMAN,*[†] D. PAUL RILLEMA,*[†] and ROBERT NOWAK[‡]

Received January 23, 1984

The preparation, spectral properties, and redox characteristics of a series of nickel(II) macrocycles are reported. The series consists of nickel(II) complexes of the $[\text{Me}_4\text{-RBzO}_2[14]\text{tetraeneN}_4]^{2-}$ ligand, where R = CH₃, H, Cl, CO₂CH₃, CO₂C-H₂CH₂CH₃, or NO₂. Two irreversible oxidations, $E_{p(1)}$ and $E_{p(2)}$, were observed that ranged from 0.39 to 0.82 V and from 0.97 to 1.34 V vs. SSCE, respectively. A reversible reduction, $E_{1/2}$, was also observed that varied from -1.51 to -1.79 V. The oxidations compared favorably to the redox behavior of a copper(II) analogue and the free base ligand and, hence, were assigned as ligand-based oxidations. The nickel(II) complex (R = CO₂CH₃) was coulometrically reduced by one electron and an ESR spectrum obtained at 77 K. Two g values, $g_{\parallel} = 2.119$ and $g_{\perp} = 2.022$, characteristic of a nickel(I) derivative were obtained. Several intense UV-visible absorptions characteristic of charge-transfer processes were observed. The bands in the near-UV region were assigned as intraligand transitions. The single band in the visible region was unique to the metal complexes, and the energy maximum, $\bar{\nu}_{\text{max}}$, of the band ranged from 576 to 601 nm. Hammett plots of $E_{p(1)}$, $E_{p(2)}$, $E_{1/2}$, and $\bar{\nu}_{\text{max}}$ ($\text{cm}^{-1} \times 10^{-3}$) vs. $2\sigma_p$ were linear and had slopes of 0.20, 0.19, 0.23, and -0.36, respectively. Plots of $\bar{\nu}_{\text{max}}$ (eV) vs. $E_{p(1)}$ and $E_{1/2}$ were also linear. On this basis and on the basis of the redox assignments of $E_{p(1)}$ and $E_{1/2}$, the visible absorption band was assigned as ligand-to-metal charge transfer.

Introduction

For some time, our work has concentrated on the design and synthesis of small molecule complexes that mimic aspects of the spectral and chemical properties of metal sites in proteins.¹⁻³ In particular, these efforts have aimed at the type II sites of copper(II) in galactose oxidase and superoxide dismutase (SOD).⁴⁻⁷ In the latter case it should be possible to design an "active" mimic since several low molecular weight copper(II) and nickel(II) complexes have superoxide dismutase activity⁸⁻¹³ and, indeed, a great deal of effort has focused on this important problem.¹⁴⁻¹⁷

A legitimate approach to an SOD active model would involve a metal complex whose redox potentials are tuned to that required to oxidize O₂⁻ in the higher oxidation state form and reduce O₂⁻ in the lower oxidation state form. The work reported here represents our efforts to design complexes with appropriate redox potentials. We report here a study of a series of Ni(II) tetraazaannulenes and their variation in redox properties as substituents are varied.

Dabrowiak and co-workers^{18,19} have reported the electrochemistry and characterized the products formed upon oxidation of the nickel(II) complex, where R = H as shown in Figure 1. The ligand systems were first reported by Jäger²⁰ and later studied by Truex and Holm.²¹ We have extended the series by derivatizing the ligand on the phenyl ring and studied the effects of varying the substituent R group upon the redox and spectral properties of the nickel(II) series.

Experimental Section

Materials. Tetraethylammonium perchlorate (TEAP) and tetrabutylammonium hexafluorophosphate (TBAH) were purchased from Southwestern Analytical Chemicals, Inc. TEAP was dried overnight at 70 °C under vacuum and used without further purification. Acetonitrile was either spectral or pesticide grade and was dried 48 h over 4-Å molecular sieves before use. Propylene carbonate was purchased from Burdick and Jackson as distilled in glass grade and dried 48 h over 4-Å molecular sieves before use. Methylene chloride and *N,N*-dimethylformamide (DMF) were reagent grade and were dried in manner similar to that of the other solvents. Nitrogen was scrubbed by passing it through a solution ~2 M in perchloric acid and ~0.2 M in chromous perchlorate generated from chromic perchlorate over zinc amalgam. All other chemicals used were reagent

grade and were used without further purification. All diamines were commercially available except methyl 3,4-diaminobenzoate and *n*-propyl 3,4-diaminobenzoate, which were prepared by Kadaba's method.²²

Preparations. $[\text{Ni}(\text{Me}_4\text{-BzO}_2[14]\text{tetraeneN}_4)]$, $[\text{Ni}(\text{Me}_4\text{-CH}_3\text{BzO}_2[14]\text{tetraeneN}_4)]$, $[\text{Ni}(\text{Me}_4\text{-ClBzO}_2[14]\text{tetraeneN}_4)]$, $[\text{Ni}(\text{Me}_4\text{-CO}_2\text{CH}_3\text{BzO}_2[14]\text{tetraeneN}_4)]$, and $[\text{Ni}(\text{Me}_4\text{-CO}_2\text{CH}_2\text{CH}_2\text{CH}_3\text{BzO}_2[14]\text{tetraeneN}_4)]$ were prepared by using a method published by Jäger.²⁰

¹H NMR (Me₂SO-*d*₆): $[\text{Ni}(\text{Me}_4\text{-CO}_2\text{CH}_3\text{BzO}_2[14]\text{tetraeneN}_4)]$, δ 2.19 (d, 12), 3.80 (s, 6), 4.93 (s, 2), 6.70 (m, 2), 7.27 (m, 4); $[\text{Ni}(\text{Me}_4\text{-CO}_2\text{CH}_2\text{CH}_2\text{CH}_3\text{BzO}_2[14]\text{tetraeneN}_4)]$, δ 1.01 (t, 6), 1.75 (q, 4), 2.17 (d, 12), 4.16 (t, 4), 4.87 (s, 2), 6.65 (m, 2), 7.30 (m, 4).

$[\text{Ni}(\text{Me}_4\text{-NO}_2\text{BzO}_2[14]\text{tetraeneN}_4)]$. The nitro-substituted macrocyclic ligand complex was prepared by a modified procedure of Jäger.²⁰ Under a N₂ atmosphere, 0.10 mol of 1,2-diamino-4-nitrobenzene and 0.050 mol of nickel(II) acetate tetrahydrate were dissolved in 100 mL of DMF and heated for 2 h at 80 °C. Then, 0.10 mol of 2,4-pentanedione in 25 mL of DMF was added dropwise. The resulting

- Bereman, R. D.; Churchill, M. R.; Shields, G. D. *Inorg. Chem.* **1979**, *18*, 3117.
- Bereman, R. D.; Shields, G. D.; Bordner, J.; Dorfman, J. R. *Inorg. Chem.* **1981**, *20*, 2165.
- Bereman, R. D.; Dorfman, J. R.; Bordner, J.; Rillema, D. P.; McCarthy, P.; Shields, G. D. *J. Inorg. Biochem.* **1982**, *16*, 47.
- Bereman, R. D.; Ettinger, M. J.; Kosman, D. J.; Kurland, R. J. *Adv. Chem. Ser.* **1977**, No. 162, 263.
- Giordano, R. S.; Bereman, R. D. *J. Am. Chem. Soc.* **1974**, *96*, 1019.
- Giordano, R. S.; Bereman, R. D.; Kosman, D. J.; Ettinger, M. J. *J. Am. Chem. Soc.* **1974**, *96*, 1023.
- Marwedel, B. J.; Kosman, D. J.; Bereman, R. D.; Kurland, R. J. *J. Am. Chem. Soc.* **1981**, *103*, 2842.
- Kimura, E.; Sakonaka, A.; Nakamoto, M. *Biochim. Biophys. Acta* **1981**, *687*, 172.
- Brigelius, R.; Hartman, H. J.; Bors, W.; Lengfelder, E.; Weser, U. *Hoppe-Seyler's Z. Physiol. Chem.* **1975**, *356*, 739.
- Brigelius, R.; Spottl, R.; Bors, W.; Lengfelder, E.; Saran, M.; Weser, U. *FEBS Lett.* **1974**, *47*, 72.
- Halliwell, B. *FEBS Lett.* **1975**, *56*, 34.
- McClune, G. J.; Fee, J. A.; McCluskey, G. A.; and Groves, J. T. *J. Am. Chem. Soc.* **1977**, *99*, 5220.
- Llan, Y. A.; Czapski, G. *Biophys. Acta* **1977**, *498*, 386.
- Amundsen, A. R.; Whelan, J.; Bosnich, B. *J. Am. Chem. Soc.* **1977**, *99*, 6730.
- Nappa, M.; Valentine, J. S.; Mikszlae, R.; Schugar, H. J. *J. Am. Chem. Soc.* **1979**, *101*, 7744.
- Pasternack, R. F.; Halliwell, B. *J. Am. Chem. Soc.* **1979**, *101*, 1026.
- Lengfelder, E.; Weser, U. *Clin. Respir. Physiol.* **1981**, *17* (Suppl.), 73.
- Dabrowiak, J. C.; Fisher, D. P.; McElroy, F. C.; Macero, D. J. *Inorg. Chem.* **1979**, *18*, 2304.
- McElroy, F. C.; Dabrowiak, J. C. *J. Am. Chem. Soc.* **1976**, *98*, 7112.
- Jäger, E.-G. *Z. Anorg. Allg. Chem.* **1969**, *364*, 177.
- Truex, T. J.; Holm, R. H. *J. Am. Chem. Soc.* **1972**, *94*, 4529.
- Kadaba, P. K. *J. Pharm. Sci.* **1974**, *68*, 1333.

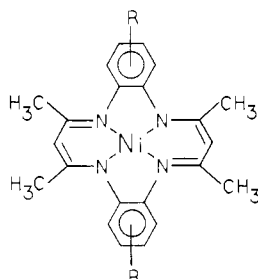
[†] North Carolina State University.

[‡] The University of North Carolina at Charlotte.

[§] Naval Research Laboratory.

Table I. Elemental Analyses of the Nickel and Copper Complexes

complex	% C		% H		% N	
	calcd	found	calcd	found	calcd	found
[Ni(Me ₄ -CO ₂ CH ₂ Bzo ₂ [14]tetraeneN ₄)]	60.37	60.01	5.08	5.10	10.83	10.71
[Ni(Me ₄ -CO ₂ CH ₂ CH ₂ CH ₃ Bzo ₂ [14]tetraeneN ₄)]	62.84	62.97	5.99	5.89	9.77	9.71
[Ni(Me ₄ -NO ₂ Bzo ₂ [14]tetraeneN ₄)]	53.79	53.42	4.11	4.31	17.11	17.53
[Cu(Me ₄ -ClBzo ₂ [14]tetraeneN ₄)]	55.64	55.71	4.25	4.26	11.80	11.92

Figure 1. [Ni(Me₄-RBzo₂[14]tetraeneN₄)].

solution was heated at reflux for 24 h, during which time a dark precipitate formed. After the suspension was cooled to room temperature, the precipitate was removed by filtration and discarded. The desired compound was isolated as a dark blue microcrystalline product by addition of water to the resulting filtrate. The solid was collected by vacuum filtration, washed with hot water and methanol, and dried under vacuum at 80 °C; yield 20%. ¹H NMR (Me₂SO-*d*₆): δ 2.05 (d, 12), 4.95 (s, 2), 6.85 (m, 2), 7.46 (m, 4).

[Cu(Me₄-ClBzo₂[14]tetraeneN₄)]. This compound was prepared by using a modified procedure from the one described for preparation of the analogous nickel(II) compound.²⁰ Under an inert atmosphere, 0.050 mol of copper(II) acetate hydrate and 0.10 mol of 4-chloro-*o*-phenylenediamine were dissolved in 200 mL of absolute ethanol and heated at 90 °C with stirring for 3 h. After dropwise addition of 0.10 mol of 2,4-pentanedione in 25 mL of absolute ethanol, the resulting solution was refluxed for 24 h. During reflux, the desired complex precipitated. The suspension was cooled to room temperature, and the blue solid was removed by filtration. It was washed with hot water and methanol, recrystallized from methylene chloride, and dried under vacuum at 80 °C; yield 28%.

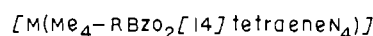
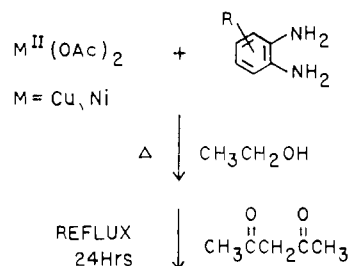
Physical Measurements. Elemental analyses were performed by Integral Microanalytical Laboratories, Raleigh, NC. Proton NMR spectra were recorded on a Varian EM-390 spectrometer in Me₂SO-*d*₆ with tetramethylsilane (Me₄S) as an internal standard. Electronic absorption spectra were obtained in acetonitrile solutions using matched 1-cm quartz cells and were recorded with a Cary 14 recording spectrophotometer. ESR spectra were recorded on a Bruker ER2000 D spectrometer, a JEOL Model PE-1X spectrometer, and a Varian E-3 spectrometer. Pitch or MnO served as ESR spectral standards.

Electrochemical properties were determined in acetonitrile, propylene carbonate, methylene chloride, and DMF solutions containing 0.10 M TEAP or 0.10 M TBAH as supporting electrolyte. Solution concentrations of the metal complexes were in the range (2–5) × 10⁻⁴ M. Cyclic voltammograms were obtained with the PAR 173 potentiostat and the PAR 175 programmer and recorded with a Houston Omnigraphic Model 2000 X-Y recorder or the IBM Model 165 X-Y recorder. The measurements were made at a Bioanalytical Systems Pt or glassy-carbon (GC) working disk electrode vs. a sodium saturated calomel electrode (SSCE). The disk electrodes were polished sequentially with 3-, 1-, and 0.25-μm diamond polishing compound followed by ultrasonic cleaning in distilled water and reagent grade acetonitrile before use. The polishing was effected with a Buehler Ltd. apparatus and ultrasonic cleaning with a Branson B-24-4 unit. Polarography was performed with a PAR 174A polarographic analyzer. Coulometry was effected with the PAR 173 potentiostat, the PAR 176 coulometer, and the PAR 370 cell system or a homemade cell system consisting of a large platinum-gauze electrode, a 150-mL beaker, and a magnetic stirrer.

Results and Discussion

Preparation of Compounds. Divalent metal complexes of the type [M(Me₄-RBzo₂[14]tetraeneN₄)] were prepared following the synthetic route shown in Scheme I. The initial

Scheme I

Table II. Redox Properties of [M(Me₄-RBzo₂[14]tetraeneN₄)] Complexes^a

M	R	$E_{p(1)}$ ^b	$E_{p(2)}$ ^b	$E_{1/2}$ ^b	$2\sigma_p$ ^c
Ni	CH ₃	0.39	0.97	-1.79	-0.34
	H	0.45	1.00	-1.73	0
	Cl	0.54	1.13	-1.63	0.46
	CO ₂ CH ₂ CH ₂ CH ₃	0.59	1.19	-1.51	0.90
	CO ₂ CH ₃	0.59	1.19	-1.51	0.90
Cu	NO ₂	0.82	1.34	<i>d</i>	1.56
	Cl	0.46	0.98	-1.29	0.54
H ₂	Cl	0.73	1.18		0.46

^a 0.1 M TEAP-acetonitrile solutions; $T = 22 \pm 2$ °C. ^b Volts vs. SSCE, ± 0.01 V; sweep rates 200 mV/s. ^c σ_p values from: Swain, C. G.; Lupton, E. C., Jr. *J. Am. Chem. Soc.* 1968, 90, 4328. Wells, P. R. "Linear Free Energy Relationships"; Academic Press: New York, 1968. ^d Irreversible.

step in the synthesis involves formation of a metal diamine complex that functioned as a template for condensation of 2,4-pentanedione to produce the desired macrocycle. Elemental analyses of previously unreported compounds given in Table I and NMR parameters given in the Experimental Section are consistent with these formulations.

The free macrocyclic ligand was obtained following the method of Jäger.²⁰ Nickel(II) was removed from the macrocycle by bubbling HCl through a solution of the appropriate nickel(II) complex, and the ligand was isolated as the hydrochloride salt. Neutralization of the solution with base yielded the free ligand.

Electrochemistry. A typical cyclic voltammogram is shown in Figure 2a. Overall, the voltammogram consists of two irreversible oxidations, a broad irreversible reduction peaking at ~ -0.50 V, which had no observable current on the scan reversal, and a reversible reduction at a more negative potential. The voltammogram is similar to that reported by Dabrowiak and co-workers.¹⁸ However, there are a number of features that we have explored in more detail.

The voltammogram was essentially the same for all complexes as the one shown in Figure 2a, regardless of the initial scan direction or the scanning rate (50–1000 mV/s). The first oxidation, $E_{p(1)}$, and the irreversible reduction are redox-coupled pairs as illustrated in Figure 2b. Scans in the +1.0 to -1.0 V range resulted in a current decrease for $E_{p(1)}$. However, the current could be restored to the value found in the overall scan if the scan range covered the +1.0 to -1.7 V

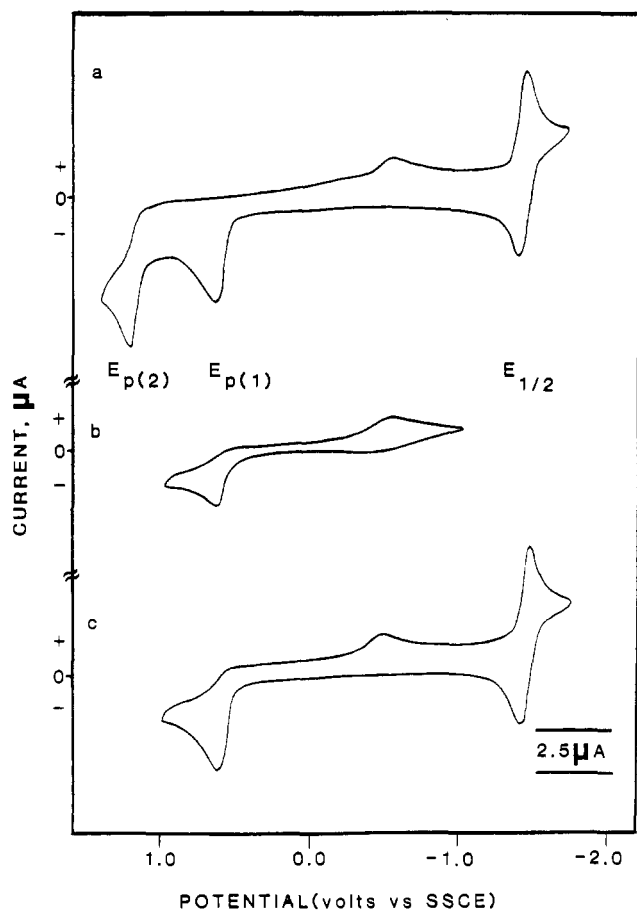


Figure 2. Cyclic voltammograms of $[\text{Ni}(\text{Me}_4\text{-CO}_2\text{CH}_2\text{CH}_2\text{CH}_3\text{Bzo}_2[14]\text{tetraeneN}_4)]$ in a 0.10 M TEAP-acetonitrile solution (sweep rate 200 mV/s): (a) +1.4 to -1.8 V vs. SSCE; (b) +1.0 to -1.0 V vs. SSCE; (c) +1.0 to -1.8 V vs. SSCE.

range as shown in Figure 2c. The overall scan shows that the second oxidation, $E_{p(2)}$, lacks a readily discernible reduction component. There is only a slight distortion in the reduction region for this voltammogram compared to the one obtained in the +1.0 to -2.0 V scan. Only the reversible reduction is observed when scans are over the 0 to -2.0 V range.

Even though the two oxidation waves are irreversible, their behavior appears to be Nernstian. The first oxidation was examined in detail. A sampled dc polarogram obtained for the nickel(II) macrocycle ($R = \text{H}$) in acetonitrile was analyzed by plotting $\log [(i_l - i_a)/i_a]$ vs. E , where i_a was the anodic current, i_l the limiting current, and E the potential at i_a . The relationship was linear, the correlation coefficient was 0.998, and the slope was 58 mV, which was consistent with a one-electron-transfer process. Also consistent with this was the 56-mV value of $E_{3/4} - E_{1/4}$.²³ Further evidence for the one-electron assignment was obtained by coulometry. Difficulties arose in conventional coulometry experiments due to deposition of solid on the electrode surface in most solvents. However, it was less severe in propylene carbonate at low substrate concentrations, so an alternate procedure was designed on the basis of this information. Aliquots (~0.10 mL) of a 1.15×10^{-3} M $[\text{Ni}(\text{Me}_4\text{-Bzo}_2[14]\text{tetraeneN}_4)]$ -propylene carbonate solution were added to 90 mL of a 0.10 M TEAP-propylene carbonate solution containing a large Pt-gauze electrode set at a potential of 0.55 V vs. SSCE (see Table III). The number of coulombs required to oxidize each added sample was determined, and a plot of $Q(\text{total})$ vs. the

Table III. Redox Properties of $[\text{Ni}(\text{Me}_4\text{-Bzo}_2[14]\text{tetraeneN}_4)]$ in Various Solvents^a

solvent	TEAP			TBAH		
	$E_{p(2)}$	$E_{p(1)}$	$E_{1/2}$	$E_{p(2)}$	$E_{p(1)}$	$E_{1/2}$
CH_2Cl_2				1.16	0.49	
CH_3CN	1.00	0.45	-1.73	1.02	0.45	-1.77
DMF	1.07	0.56	-1.67	1.28 ^b	0.58	-1.67
propylene carbonate	1.00	0.45	-1.75	1.05	0.48	-1.75

^a Similar conditions, error limits, and units as given in Table II.

^b The second oxidation is marked by an irreversible, multielectron wave that peaks at 1.28 V.

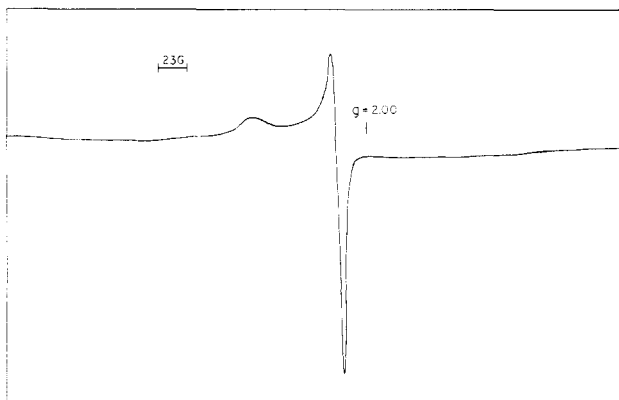


Figure 3. ESR spectrum of one-electron-reduced $[\text{Ni}(\text{Me}_4\text{-CO}_2\text{CH}_3\text{Bzo}_2[14]\text{tetraeneN}_4)]$ at 77 K in a frozen 0.10 M TEAP-acetonitrile matrix.

volume of added reagent was constructed. The plot was linear, with a slope corresponding to an n value of 1.1. Both $E_{p(2)}$ and the reversible reduction have currents similar to $E_{p(1)}$ and, hence, are also assigned as one-electron processes. The difference in peak potentials for the reduction couple was 75 mV—a value often found in nonaqueous systems for reversible one-electron processes.²⁴

The reversible reduction is associated with the metal center.¹⁸ To confirm this, $[\text{Ni}(\text{Me}_4\text{-CO}_2\text{CH}_3\text{Bzo}_2[14]\text{tetraeneN}_4)]$ (1.0×10^{-3} M) was reduced electrochemically in 0.10 M TEAP-acetonitrile solution. After reduction ($n = 1$) was effected at -1.6 V, the solution was transferred to an ESR tube and frozen at 77 K, and the spectrum shown in Figure 3 was obtained. The spectrum contains the general features previously associated with nickel(I) complexes. The g_{\parallel} (2.119) and g_{\perp} (2.022) values are somewhat lower than those previously reported for nickel(I) macrocycle complexes.²⁵⁻²⁷ However, the g values are greater than those associated with ligand-centered reductions and, hence, are assigned to a nickel(I) species. Dabrowiak et al.¹⁸ encountered a similar situation for the one-electron-reduced nickel(II) parent ($R = \text{H}$) compound and assigned three g values ($g_x = 2.137$, $g_y = 2.03$, $g_z = 2.02$) on the basis of a rhombic model for the nickel(I) macrocycle. A similar interpretation could be made for the above ester derivative.

Two irreversible oxidations were observed for $[\text{H}_2(\text{Me}_4\text{-ClBzo}_2[14]\text{tetraeneN}_4)]$ in 0.10 M TEAP-acetonitrile as shown in Figure 4. The two oxidation waves, $E_{p(1)}$ and $E_{p(2)}$, are observed in the same region as for the complex shown in Figure 2. Repetitive scanning from 0 to +1.3 V resulted in passivation of the electrode due to solid formation on the

(23) Bard, A. J.; Faulkner, L. R. *Electrochemical Methods, Fundamentals and Applications*; Wiley: New York, 1980.

(24) Brown, G. M.; Hopf, F. R.; Meyer, T. J.; Whitten, D. G. *J. Am. Chem. Soc.* **1975**, *97*, 5385.

(25) Lovecchio, F. V.; Gore, E. S.; Busch, D. H. *J. Am. Chem. Soc.* **1974**, *96*, 3109.

(26) Gagne, R. R.; Ingle, D. M. *Inorg. Chem.* **1981**, *20*, 420.

(27) Lewis, J.; Schröder, M. *J. Chem. Soc., Dalton Trans.* **1982**, 1085.

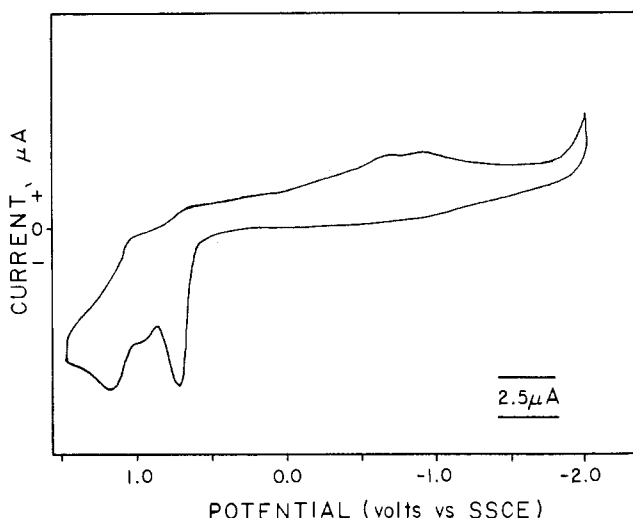


Figure 4. Cyclic voltammogram of $[H_2(Me_4-ClBzo_2[14]tetraeneN_4)]$ in a 0.10 M TEAP-acetonitrile solution from +1.5 to -2.0 V vs. SSCE (sweep rate 200 mV/s).

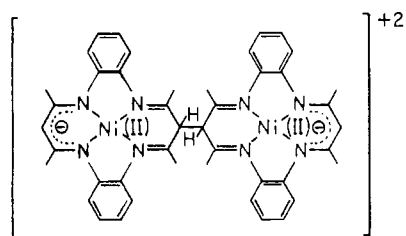


Figure 5. Proposed dimer formed upon oxidation of nickel(II) tetraazaannulene.

electrode surface. This same phenomenon has also been observed for oxidation of *o*-phenylenediamine.²⁸ The small wave between $E_{p(1)}$ and $E_{p(2)}$ may be a prewave associated with deposition of compound on the electrode surface. Prewaves are often found in cases where materials are surface bound.²⁹ Reductions that occurred at a more negative potential than -2.0 V vs. SSCE were not investigated due to experimental difficulties, although Kadish et al.^{30,31} reported that the potential for reduction of $[H_2(Me_4-Bzo_2[14]tetraeneN_4)]$ in DMF with 0.1 M tetrabutylammonium fluoroborate as the electrolyte was <-2.20 V vs. SLCE (saturated lithium calomel electrode).

The one-electron oxidation of the parent nickel(II) macrocycle (R = H) has been reported to result in the formation of a very interesting dimer¹⁹ as shown in Figure 5. Two complexes were joined at the δ position of the diiminate framework. The dimer could be deprotonated to give a second dimer that was similar in many respects to the starting complex.

The electrochemical data obtained for the series (R = CH₃, H, CO₂CH₃, CO₂CH₂CH₂CH₃, Cl, NO₂) are given in Table II. Potentials are listed as peak values for the two oxidation steps and as $E_{1/2}$ values for the reversible reduction. The series contains macrocycles with various electron donor and withdrawing groups that have different σ_p values.³² Plots of $E_{p(1)}$,

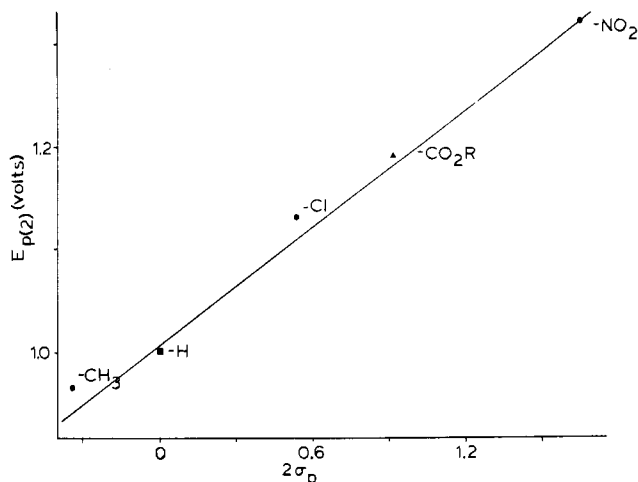


Figure 6. Hammett plot of $E_{p(2)}$ vs. $2\sigma_p$ (corr = 0.99, slope = 0.19) illustrating the dependence of redox potentials on σ_p .

Table IV. Electronic Absorption Bands for $[Ni(Me_4-RBzo_2[14]tetraeneN_4)]$ and $[H_2(Me_4-ClBzo_2[14]tetraeneN_4)]^a$

substituent	$\bar{\nu},^a \text{ cm}^{-1} \times 10^{-3} (\epsilon)$	other transitions ($\bar{\nu}, \text{ cm}^{-1} \times 10^{-3} (\epsilon)$)
H	17.15 (6250) ^c	26.54 (36 250), 26.81 (20 000) 29.94 (7500), 37.74 (27 100) 43.68 (27 500)
CH ₃	17.36 (1600)	25.45 (8600), 42.74 (17 700)
Cl	17.07 (6700) ^c	23.26 (14 600), 25.32 (41 000) 37.31 (31 800)
CO ₂ CH ₂ CH ₂ CH ₃	16.89 (8700)	23.53 (24 500), 37.74 (40 000)
NO ₂	16.64 (8800)	21.19 (19 000), 24.03 (22 500) 27.03 (16 500)
H ₂ L		28.90 (29 100), 36.36 (10 400) 39.22 (10 900)

^a Spectra were obtained for 10^{-4} M solutions in acetonitrile.

^b $22 \pm 2^\circ \text{C}$; $\bar{\nu}$, ± 0.02 ; ϵ , $\pm 1\%$. ^c See ref 20.

$E_{p(2)}$, and $E_{1/2}$ vs. $2\sigma_p$ are linear, as shown in the representative example in Figure 6, with correlation coefficients of 0.98, 0.99, and 0.99, respectively. The slopes fall in the 0.19–0.23 range, which is intermediate between slopes of 0.07 found for macrocycles³³ and metalloporphyrins³⁴ containing remote substituents and 0.50 for similar systems containing substituents bound to a skeletal carbon atom of the macrocycle ring.^{33,35} However, as found here, Giraudeau and co-workers³⁶ found similar slopes for metalloporphyrins with β substituents located on the pyrole residues of the porphyrin ligand. The data reported here are consistent with oxidation at the δ -carbon atom of the diiminate framework of the macrocyclic ligand and reduction at the metal center.

Solvent and Electrolyte Dependence of Redox Potentials.

Data in Table III indicate that redox potentials are both solvent and electrolyte dependent. The redox potentials for a given process vary approximately 0.1 V in the solvents and elec-

(28) Heineman, W. R.; Wieck, H. J.; Yacynych, A. M. *Anal. Chem.* **1980**, *52*, 345 and references therein.

(29) Denisevich, P.; Abruna, H. D.; Leidner, C. R.; Meyer, T. J.; Murray, R. W. *Inorg. Chem.* **1982**, *21*, 2153. Ellis, C. D.; Murphy, W. R.; Meyer, T. J. *J. Am. Chem. Soc.* **1981**, *103*, 7480. Ellis, C. D.; Margerum, L. D.; Murray, R. W.; Meyer, T. J. *Inorg. Chem.* **1983**, *22*, 1283.

(30) Kadish, K. M.; Schaeper, D.; Bottomley, L. A. *J. Inorg. Nucl. Chem.* **1980**, *42*, 469.

(31) Kadish, K. M.; Bottomley, L. A.; Schaeper, D. *Inorg. Chim. Acta* **1979**, *36*, 219.

(32) As pointed out elegantly by Kadish et al. in ref 34d, the exact choice of which Hammett parameter to use, i.e. σ_p , σ^+ , σ^- , etc., is not clear. We have chosen σ_p because the correlations are linear and it offers comparisons to the widest range of literature data.

(33) Steeky, J. A.; Pillsbury, D. G.; Busch, D. H. *Inorg. Chem.* **1980**, *19*, 3148.

(34) (a) Kadish, K. M.; Morrison, M. M. *J. Am. Chem. Soc.* **1976**, *98*, 3326. (b) Kadish, K. M.; Morrosion, M. M. *Inorg. Chem.* **1976**, *15*, 980. (c) Walker, F. A.; Beroiz, D.; Kadish, K. M. *J. Am. Chem. Soc.* **1976**, *98*, 3484. (d) Malinski, T.; Chang, D.; Bottomley, L. A.; Kadish, K. M. *Inorg. Chem.* **1982**, *21*, 4248. (e) Rillema, D. P.; Nagle, J. K.; Barringer, L. F., Jr.; Meyer, T. J. *J. Am. Chem. Soc.* **1981**, *103*, 56.

(35) Kadish, K. M.; Morrison, M. M. *Bioinorg. Chem.* **1977**, *7*, 107.

(36) Giraudeau, A.; Callot, H. J.; Gross, M. *Inorg. Chem.* **1979**, *18*, 201. Giraudeau, A.; Callot, H.; Jordan, J.; Ezhar, I.; Gross, M. *J. Am. Chem. Soc.* **1979**, *101*, 3857.

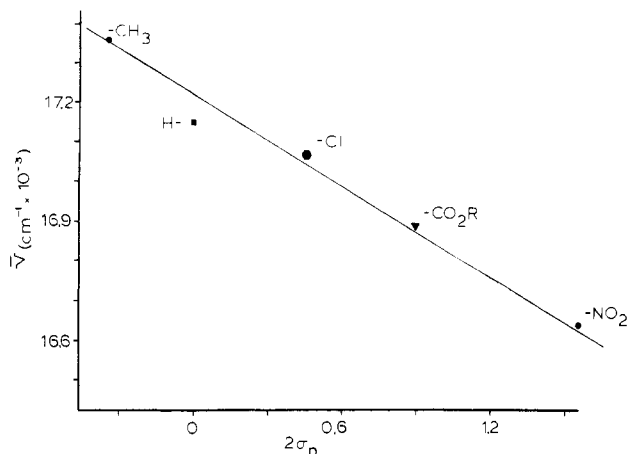


Figure 7. Correlation between the energy maximum ($\text{cm}^{-1} \times 10^{-3}$) of the visible transition and the Hammett σ_p parameter (corr = 0.99, slope = -0.36).

trolytes utilized in these studies. In DMF, the potentials are shifted ~ 0.1 V more positive than in acetonitrile but are somewhat less positive than reported by Kadish and co-workers^{30,31} where potentials were determined in DMF containing tetrabutylammonium fluoroborate (TBAT) and were referenced with respect to a saturated lithium calomel electrode (SLCE). The potentials for the oxidation in CH_2Cl_2 are consistent with those reported by Dabrowiak et al.,¹⁸ after taking into account that the reference these workers used was an aqueous Ag/AgCl electrode. The dependence of redox potentials for nickel(II) porphyrins on solvent and electrolyte was recently reported by Kadish and co-workers.³⁷ Since tetraazaannulenes are models for porphyrins, similar behavior is not unexpected.

Electronic Spectra. Absorption spectra of the complexes and free base ligand ($R = \text{Cl}$) were examined over the 220–800 nm range, and the results are summarized in Table IV. The complexes exhibit one intense absorption band in the visible and several intense absorptions in the near-UV regions of the spectrum. The higher energy bands fall in the region characteristic of the free base ligand and apparently are intraligand electronic transitions. The band in the visible is unique to the metal complexes and has energy maxima ranging from 576 to 601 nm, with extinction coefficients of $1600\text{--}8800 \text{ M}^{-1} \text{ cm}^{-1}$. These extinction coefficients are indicative of charge-transfer absorptions, the source of which will be discussed in more detail below.

The effect of the substituent on the transition energy maximum of the visible band was examined by means of a Hammett plot. Figure 7 shows that the relationship between $\bar{\nu}_{\max}$ and $2\sigma_p$ is linear, with a slope of -0.36 ($= -0.72/\sigma_p$) and a correlation coefficient of 0.99. Interestingly, Busch and co-workers³³ found a positive slope of value $1.5/\sigma_p$ for other nickel(II) tetraaza N_4 macrocycles where the correlation was made with d–d band maxima. Obviously, a different orbital must be involved here to account for the negative slope found for the optical transition dependence with substituents of these tetraazaannulenes.

The origin of the low-energy charge-transfer transition can perhaps be understood by considering the dependence of $\bar{\nu}_{\max}$ on the redox potentials. Both $E_{p(1)}$ and $E_{1/2}$ linearly track $\bar{\nu}_{\max}$,

but at slightly different rates. The slope of $\bar{\nu}_{\max}$ vs. $E_{p(1)}$ is -0.23 (corr = 0.98); the one for $\bar{\nu}_{\max}$ vs. $E_{1/2}$ is -0.19 (corr = 0.97).³⁸ Clearly, both the oxidation and reduction of the complexes correlate with the optical transition in the visible.

Arguments can be raised regarding the ground-state and excited-state orbital assignments that correspond to the optical transition. The lowest occupied orbital appears to be ligand centered. This is consistent with the chemistry of dimer formation through the diiminate framework of the macrocycle following oxidation¹⁹ and the similarity of the redox behavior of the free base ligand compared to that of the nickel(II) complex. It is interesting to note that this is similar to the reported behavior of tetraphenylporphyrin and its nickel(II) complex, where oxidation of the free ligand occurs at 1.08 V³⁶ and oxidation of the nickel(II) complex occurs at 1.05 V³⁶ vs. SCE in CH_2Cl_2 with a tetraalkylammonium salt as the electrolyte. Considerable effort has been expended to show that the oxidation of nickel(II) porphyrins results in formation of a radical cation, rather than a nickel(II) complex.³⁷ Further evidence for ligand oxidation can be made by comparing potentials for oxidation of the copper(II) complex to its nickel(II) analogue in Table II. $E_{p(1)}$ and $E_{p(2)}$ occur in the same potential region but are shifted ~ 0.1 V more negative. Since copper(III) is an unlikely oxidation state, the shift is undoubtedly due to the electronic changes brought about by the different metal centers. There is a much larger shift (~ 0.3 V) in the positive direction for reduction of the copper complex, which is consistent with reduction of copper(II) to copper(I). Copper(I) is a viable oxidation state, and ESR evidence for reduction of nickel(II) certainly corroborates the point of a metal-centered reduction for the complexes in this potential region. Hence, the optical transition most likely corresponds to movement of the electron from a filled molecular orbital on the ligand to an unoccupied molecular orbital associated with the metal.

Conclusion. The results indicate that the redox behavior of the tetraazaannulene complexes can be tuned by the appropriate choice of substituent(s) bound to the macrocyclic ligand. It is also clear from other work^{33–36} that the magnitude of this effect can be controlled by the precise location of the substituent. The metal center also makes a difference. According to the data in Table II, the potential for reduction of the copper complex ($R = \text{Cl}$) is shifted to a more favorable value of -1.29 V compared to -1.63 V for the nickel(II) analogue.

Acknowledgment. This work was supported by the Office of Naval Research, the North Carolina Biotechnology Center, and the foundation of the University of North Carolina at Charlotte. D.P.R. also thanks the American Society of Engineering Education for a 1983 Summer Faculty Fellowship with the Department of the Navy. This is paper no. 1 from the North Carolina Biomolecular Engineering and Materials Applications Center.

Registry No. [Ni(Me₄-CO₂CH₃Bzo₂[14]tetraeneN₄)], 92396-70-8; [Ni(Me₄-CO₂CH₂CH₂CH₃Bzo₂[14]tetraeneN₄)], 92396-71-9; [Ni(Me₄-NO₂Bzo₂[14]tetraeneN₄)], 92396-72-0; [Cu(Me₄-ClBzo₂[14]tetraeneN₄)], 92396-73-1; [Ni(Me₄-CH₃Bzo₂[14]tetraeneN₄)], 74834-16-5; [Ni(Me₄-Bzo₂[14]tetraeneN₄)], 51223-51-9; [Ni(Me₄-ClBzo₂[14]tetraeneN₄)], 92396-74-2; [H₂(Me₄-ClBzo₂[14]tetraeneN₄)], 92396-75-3; [Ni(Me₄-CO₂CH₃Bzo₂[14]tetraeneN₄)]⁻, 92396-77-5; methyl 3,4-diaminobenzoate, 36692-49-6; *n*-propyl 3,4-diaminobenzoate, 92396-76-4; 1,2-diamino-4-nitrobenzene, 99-56-9; 4-chloro-*o*-phenylenediamine, 95-83-0; 2,4-pentanedione, 123-54-6.

(37) Chang, D.; Malinski, T.; Ulman, A.; Kadish, K. M. *Inorg. Chem.* **1984**, *23*, 817 and references therein.

(38) The correlation was made with $\bar{\nu}_{\max}$ expressed in eV.